Microsystem Technologies
https://doi.org/10.1007/s00542-025-05963-5

TECHNICAL PAPER

A frequency selective surface (FSS) based on a reconfigurable MEMS switch for GNSS L1-band

Massimo Donelli[1,4,5] · Mohammedhusen Manekiya[1] · Irene Dal Chiele[1] · Girolamo Tagliapietra[2] · Jacopo Iannacci[2] · Koushik Guha[3]

Received: 18 May 2025 / Accepted: 21 September 2025

Abstract
This paper presents a tunable Frequency Selective Surface (FSS) for the L1-band of navigation frequencies that utilises a MEMS switch. The reconfigurable frequency-selective electromagnetic filter, achieved by combining hard magnetic materials with microelectromechanical systems (MEMS), provides a novel approach to reconfigurable frequency-selective surfaces (FSS). By incorporating magnetically actuated dipole components that can tilt away from the base surface, we can adjust the operating frequency of the FSS without physically modifying the size of the dipole components. The 9×9 array, measuring 365 mm, consists of plates made from Rogers RO3003 material, each with dimensions of $531.2 \times 531.2 \times 8.768$ mm, layered with a 0.03 mm-thick copper conductor (Cu). The proposed system features a cross dipole printed on a Rogers-RO3003 substrate, with a MEMS switch placed between one of the dipole arms to adjust its length. The MEMS switch facilitates frequency tuning by altering the length of a rectangular dipole. This phase modulation technique enables the steering of reflected waves, thereby enhancing beam resolution and coverage, while allowing the intelligent reflecting surface (IRS) to control the reflection of reflection. The presented reconfigurable FSS design has effectively demonstrated the ability to tune its resonant frequency for the L1-band without physically changing its dimensions. The design was assessed using the commercial simulation software CST, and the numerical results corroborate the findings, thereby confirming its effectiveness.

Keywords Frequency selective surface (FSS) · RF-MEMS · L1 frequency band · GNSS

1 Introduction

In recent years, several methods have been reported for designing reconfigurable antennas. These methods include steering the beam by introducing parasitic elements in either stacked or planar configurations, exciting different working modes of a single antenna, and reconfiguring the antenna's electrical structure. Frequency-selective surfaces (FSS) have emerged as a viable option for reconfiguring the properties of antennas. An FSS can be electronically adjusted using active devices, such as varactors or PIN diodes, allowing control over its transmission and reflection

✉ Mohammedhusen Manekiya
m.manekiya@unitn.it

Massimo Donelli
massimo.donelli@unitn.it

Irene Dal Chiele
irene.dalchiele@unitn.it

Jacopo Iannacci
iannacci@fbk.eu

Koushik Guha
koushik@ece.nits.ac.in

[1] Department of Civil, Environmental and Mechanical Engineering (DICAM), University of Trento, Trento 38123, Italy

[2] Center for Sensors and Devices (SD), Fondazione Bruno Kessler (FBK), Trento, Italy

[3] Department of Electronics and Communication Engineering, National Institute of Technology (NIT), Silchar, Assam 788010, India

[4] Center for Security and Crime Sciences, University of Trento and Verona, Verona, Italy

[5] Radiomics Laboratory, Department of Economy and Management, University of Trento, Trento 38100, Italy

Published online: 06 October 2025

characteristics (Rana et al. 2023; Mamedes 2021). By modifying the equivalent geometry, the frequency response and radiation pattern of the antenna can also be altered. They can substantially enhance the capacity and coverage of wireless networks. Future communication systems beyond 5G and 6G are expected to include smart propagation environments where FSS can play a pivotal role. FSS consists of various small unit cells, each incorporating a tuning mechanism that reflects or transmits incoming waves in the desired direction. The impedance of these unit cells can be adjusted using PIN diodes (Mamedes 2021), varactor diodes, microelectromechanical systems (MEMS), thermal elements, and other approaches (Mamedes 2021; Mansutti 2020; Sharma 2022). Some research (Ghosh 2020; Schoenlinner et al. 2004)has explored the development of MEMS-enabled frequency-selective surfaces (FSS) for various applications. MEMS technology allows for tunable FSS structures that can switch or vary their resonance frequencies. Despite the widespread use of SAW and BAW filters, challenges persist in scaling these technologies to operate efficiently at frequencies beyond 6 GHz (Assylbekova et al. 2023; Ansari 2019). SAW filters face limitations due to fabrication complexity and increased ohmic losses at higher frequencies, while BAW filters encounter degradation in electromechanical coupling and quality factors as device dimensions shrink (Assylbekova et al. 2023; Ansari 2019; Loebl 2004). Recent research has explored novel materials such as scandium-doped aluminum nitride (AlScN) and lithium niobate (LiNbO3) thin films, as well as innovative device architectures like periodically poled piezoelectric films and transferred thin-film platforms, to overcome these limitations (Izhar 2024; Barrera 2024; Chen 2023). However, a knowledge gap remains regarding the integration of these advancements into devices that simultaneously improve performance, reduce cost, and enhance functionality compared to traditional bulk and surface acoustic wave filters (Stettler and Villanueva 2025; Hakim 2023; Yang 2024). In (Kim 2024; Safari et al. 2015), a capacitively loaded slot FSS with a MEMS bridge was demonstrated, achieving resonance frequency variation from 8.54 to 10.26 GHz (Kiani 2011). proposed a 60 GHz FSS with MEMS switches, capable of 30 dB transmission switching (Coutts 2007). introduced a MEMS-tunable FSS monolithically integrated on a flexible Kapton substrate, switching between Ku and Ka bands. They also developed a novel MEMS process for fabricating devices on rigid-flex organic substrates, demonstrating both FSS and electromagnetic-bandgap structures. These advancements enable the development of reconfigurable multi-band reflector antennas and conformal radomes for high-frequency operations. The research demonstrates a strong correlation between simulated and measured results, indicating the feasibility and potential of MEMS-enabled FSS technology. This highlights the importance of improving both usability and beam steering capabilities in Reconfigurable Intelligent Surface (RIS) setups. Maintaining precise phase differences among the unit cells of the RIS is essential to ensure optimal communication performance. MEMS-enabled frequency-selective surfaces (FSS) have been developed across various frequency bands, offering tunable and reconfigurable electromagnetic properties (Kim 2024; Safari et al. 2015). In this paper, we specifically focus on the L1 band of FSS, which is particularly relevant for navigation and communication systems. The integration of MEMS technology with FSS significantly enhances reconfigurability for multi-band reflector antennas and tunable conformal radomes in high-frequency applications. Recent advancements have concentrated on developing switchable FSS using MEMS and diode technologies, which present promising applications in wireless communications, radar systems, and electromagnetic shielding. The capability to dynamically control transmission and reflection properties at various frequencies exemplifies the versatility and potential of these MEMS and diode-based FSS designs. This paper presents a tunable Frequency Selective Surface (FSS) that utilises a MEMS switch, which enables frequency tuning through the adjustment of a rectangular dipole length, as presented in (Safari et al. 2015). This phase modulation technique facilitates the steering of reflected waves, thereby improving beam resolution and coverage while allowing the intelligent reflecting surface (IRS) to dictate the direction of reflection. The design was meticulously analysed, and the numerical findings align with experimental results, validating its effectiveness. The subsequent section will discuss the design of the Frequency Selective Surface, including numerical and experimental assessments that affirm the potential of the proposed FSS design.

2 Frequency selective surface design

The fundamental characteristic of a passive reflect-array is the correlation between geometric parameters and reflection phase. Changes to these parameters modify the reflection phase, which delineates the design curve from which the patch element dimensions are derived, considering their distance from the feed centre. Increasing the electrical length of the patch lowers the resonant frequency, necessitating miniaturisation of the antenna to achieve resonance at the desired frequency. This methodology enables reflect-array elements with identical side lengths, effectively reducing the spacing between them and optimising scan angles for beam-scanning applications. Reflect-array antennas combine two distinct technologies: phased arrays and conventional reflectors. A typical reflect-array consists of multiple

radiators that impart a specified phase to the incident field from a feed or various feeds, reradiating the signal into free space. The design of a frequency-selective surface (FSS) aimed at a specific resonant frequency involves several critical considerations, including the dimensions of the conductive elements, unit-cell periodicity, the thickness of the supporting surface, and the dielectric properties (Kiani 2011; Coutts 2007). The size of the conductive elements has a direct impact on the operating frequency, while the dielectric material affects both the frequency and bandwidth. Accurate determination of geometry necessitates both empirical and numerical simulations due to the intricate interactions and diminutive elements involved. The largest dimension of the periodic element establishes the resonant frequency. For a long, narrow rectangular dipole, resonance is achieved when the wavelength is approximately double the dipole length, resulting in coherent re-radiation when multiple dipoles are arranged. A significant disparity between dipole length and half-wavelength may induce signal transparency through the frequency-selective surface (FSS) (Cheng 2009).

The fundamental characteristic of a passive reflect-array is the correlation between geometric parameters and reflection phase. Changes to these parameters modify the reflection phase, which delineates the design curve from which the patch element dimensions are derived, considering their distance from the feed centre. Increasing the electrical length of the patch lowers the resonant frequency, necessitating miniaturisation of the antenna to achieve resonance at the desired frequency. This methodology enables reflect-array elements with identical side lengths, effectively reducing the spacing between them and optimising scan angles for beam-scanning applications. Reflect-array antennas combine two distinct technologies: phased arrays and conventional reflectors. A typical reflect-array consists of multiple radiators that impart a specified phase to the incident field from a feed or various feeds, reradiating the signal into free space.The design of a frequency-selective surface (FSS) aimed at a specific resonant frequency involves several critical considerations, including the dimensions of the conductive elements, unit-cell periodicity, the thickness of the supporting surface, and the dielectric properties (Kiani 2011; Coutts 2007). The size of the conductive elements has a direct impact on the operating frequency, while the dielectric material affects both the frequency and bandwidth. Accurate determination of geometry necessitates both empirical and numerical simulations due to the intricate interactions and diminutive elements involved. The largest dimension of the periodic element establishes the resonant frequency. For a long, narrow rectangular dipole, resonance is achieved when the wavelength is approximately double the dipole length, resulting in coherent re-radiation when multiple dipoles are arranged. A significant disparity between dipole length and half-wavelength may induce signal transparency through the frequency-selective surface (FSS) (Cheng 2009).

Furthermore, transmission losses may arise due to the supporting dielectric, and critical dielectric parameters, such as relative permittivity and thickness, influence these losses. A comprehensive understanding of these effects is crucial for designing high-quality FSS, necessitating compensation for any potential attenuation that may occur (Cheng 2009). The substrate will influence the frequency response in a predictable way, as long as its permittivity is accurately characterized. This downward shift in frequency corresponds to the factor $1/\sqrt{(\in_r +1)/2}$for a substrate that is at least one-tenth of a wavelength thick (Munk 2000). Consequently, a dipole-element frequency-selective surface (FSS) design must account for the attenuation caused by the supporting dielectric material to achieve the desired resonance frequency f_r. This involves designing dipole elements for a compensated resonance frequency f_{dipole}, expressed by the equation.

$$f_r = f_{dipole}/\sqrt{(\in_r +1)/2}$$

Moreover, an increase in dielectric loss resulting from greater thickness will influence the characteristics of the frequency response (Munk 2000). In this study, we have developed a design for frequency tuning that spans the L1-band without physically altering the dimensions. The configuration of the proposed reconfigurable frequency-selective surface unit is depicted in Fig.1. This design features two dipole elements arranged in a cross formation. As illustrated in Fig. 2, the right-side dipole is shorter than the left-side dipole, which is narrower and connected to two independent MEMS switches. When a vertically polarized incoming wave interacts with a half-wave dipole [see Fig. 2], the dipole element will resonate, regardless of the angle of incidence with respect to its width. When the incidence of the L1-band is oblique in relation to the length of the dipole element, effective resonance will not occur, as the projected length of the dipole in this direction (along the line of incidence) is less than the necessary wavelength. As a result, the attenuation at the specified resonant frequency decreases substantially when incoming waves strike at angles oblique to the length of the dipole. We will leverage this angle-of-incidence dependency as a valuable mechanism to achieve functional reconfiguration capabilities. The proposed system comprises a cross dipole printed on a Rogers-RO3003 substrate, incorporating a MEMS switch between one of the dipole arms to modify its length. By adjusting the distance between the metastrips, it can reflect electromagnetic waves at various angles. Each unit cell utilises four MEMS

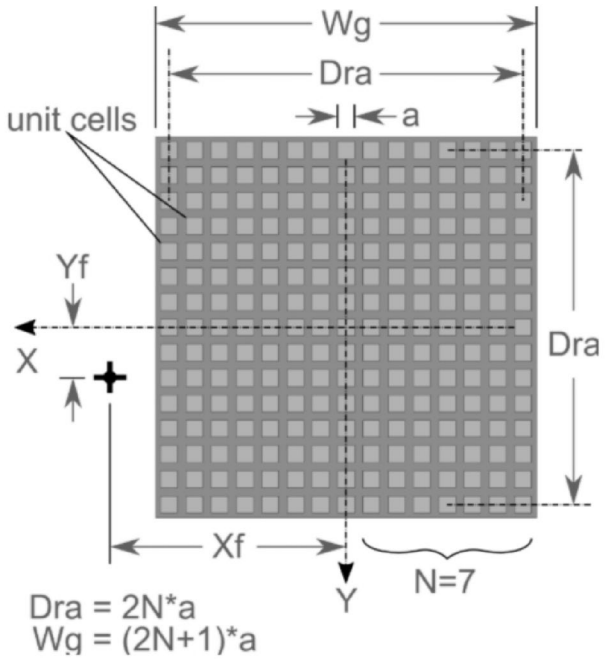

Fig. 1 Schema of the Frequency Selective Antenna

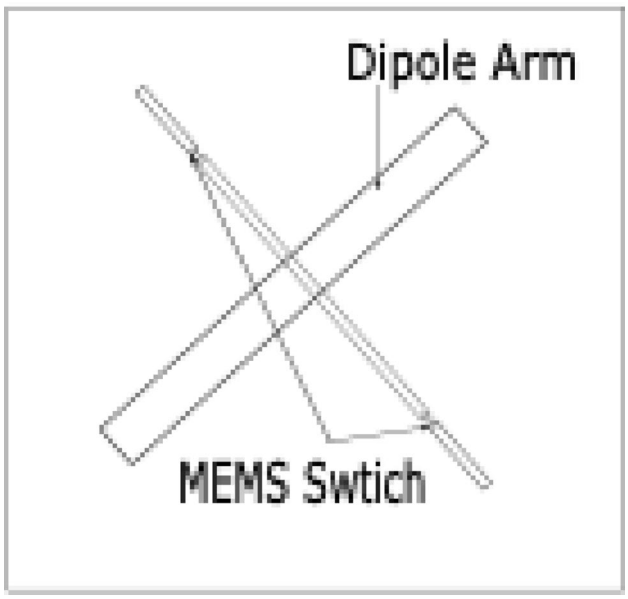

Fig. 2 Schema of the single element FSS antenna

switches for phase modulation at 1.5 GHz. Our novel approach to achieving FSS reconfigurability for dual-band operation is to individually tilt each dipole element, without tilting the substrate, as shown in Fig. 2. For a transmission signal normally incident on the supporting surface, a dipole tilt of 0 corresponds to the dipole being orthogonal to the incident wave. Doing so will allow the projected surface area of each dipole element to vary according to the degree of tilt, approximating a dipole element with a variable length (see Fig. 2). By accurately controlling the MEMS switch, a unique means of tuning the resonance frequency of an FSS is achieved. Although the reflection coefficients increase for both the on and off states, a high capacitance occurs in the off state due to the gap between the dipole, which diminishes when the MEMS is activated. The E-field is focused near the dipole's gap. When the MEMS is off, a high capacitance results from the gap between the dipole, while this capacitance diminishes when the MEMS is activated.

3 Numerical assessment and results

This section presents a detailed numerical and experimental evaluation of the proposed reconfigurable frequency selective surfaces (FSS). In this regard, various simulations were conducted to assess the efficacy of a single unit cell of the FSS in measuring reflection in response to the on-off states of the MEMS switch. The numerical evaluations were conducted using CST Studio. As detailed in the design section, a Rogers RO3003 substrate with a dielectric constant (permittivity) of $\varepsilon = 3$ was utilized, featuring copper conductors with a thickness of 0.03 mm. The substrate height is initially set at 8.763 mm. Each unit cell comprises two dipoles arranged in a cross configuration, consisting of a broader dipole on the right side and a narrower, tilted dipole on the left side, which incorporates a Micro-Electro-Mechanical Systems (MEMS) switch at its terminus. The dimensions of a single unit cell of the FSS are 59.96×59.96 mm, and the complete structure forms a 9×9 array, measuring 531.2×531.2 mm. The cross-shaped dipole configuration also facilitates the achievement of polarisation while tuning the frequency. The measured simulated results for the frequency-selective unit are illustrated in Figs. 3 and 4, which present the electric field (E-field) directivity and gain with the MEMS switch in the on state for the FSS unit.

The reflectarray exhibits optimal the number of elements, N, is equal to or exceeds seven in the design. For a centre-fed configuration radiating broadside, this configuration corresponds to a gain of approximately 15 dBi, accompanied by a beamwidth of approximately 34.8° in both the E- and H-planes. Typically, the side lobe level (SLL) is 14 dB or better below the main beam. However, designs featuring N equal to four or five elements may experience a degradation in the SLL.

The impedance characteristics of this antenna are contingent upon the feed antenna employed. In the context of a horn antenna, the impedance will likely be dictated by the coaxial-to-waveguide transition utilised in the physical implementation of the antenna. The design curve is derived from simulations of a single element (unit cell) using a Floquet port in CST Studio Suite. It is observed that

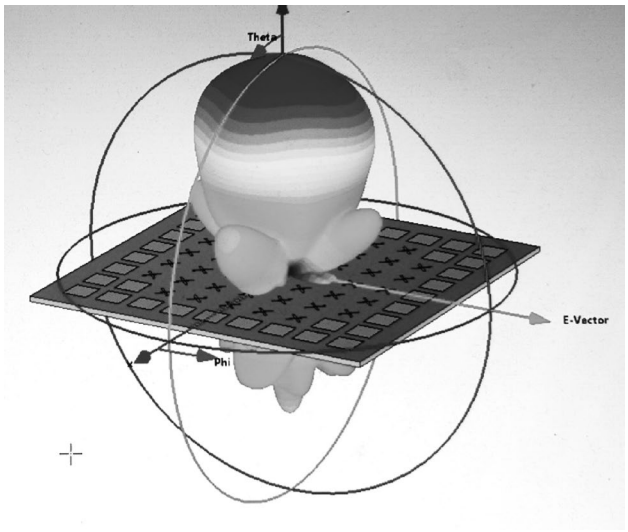

Fig. 3 Simulated Electric Far Field pattern, Directivity in E plane at 1.5 GHz

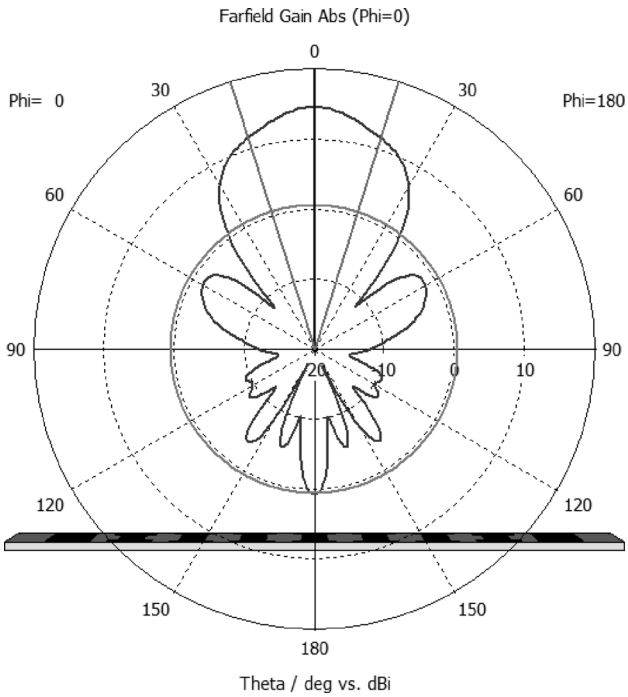

Fig. 4 Simulated Electric Far Field pattern Gain in E plane at 1.5 GHz

the reflected phase depends on the electrical thickness of the substrate. Figures 5 and 6 illustrate the core functional attributes of the proposed reconfigurable MEMS-based Frequency Selective Surface (FSS) designed for GNSS L1-band applications. Figure 5 depicts the simulated electric far-field gain pattern at 1.5 GHz upon activation of the MEMS switches, demonstrating the device's ability to direct the main reflected beam away from broadside by 20°. This confirms the FSS's capabilities in beamforming and reconfigurability. The beam steering is achieved through

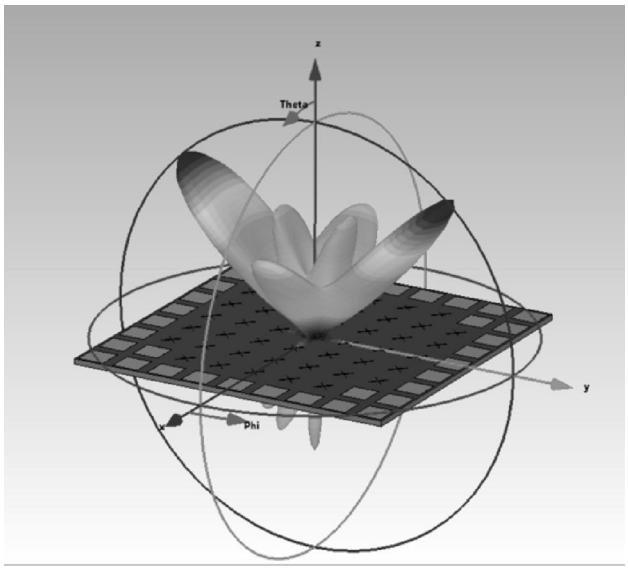

Fig. 5 Simulated Electric Far Field pattern Gain when the MEMS switches are activated at 1.5 GHz

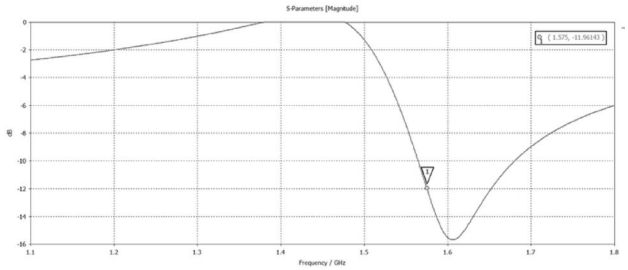

Fig. 6 Simulated S11 Parameter of the reconfigurable MEMS-Based FSS across the L1 Band

precise phase modulation enabled by integrated MEMS switches, which allow for dynamic redirection of reflected electromagnetic waves to improve signal coverage and reduce multipath interference—features particularly valuable for communication and navigation systems. Equally, Fig. 6 shows the simulated S11 reflection coefficient across the L1 frequency band, highlighting the influence of MEMS switching on the resonant behavior of the device. The S11 describes a tunable resonance that depends on the states of the MEMS switches, showing the FSS's capacity for dynamic frequency adaptation within the L1 band. Overall, these results demonstrate that MEMS integration provides versatile control over both beam direction and frequency response, emphasizing the potential and effectiveness of the developed FSS in advanced electromagnetic applications. Nevertheless, the sharpness of the filter and the degree of attenuation progressively diminish when the MEMS switch is deactivated. Within the frequency range of 1 to 4 GHz, the conductors exhibit minimal to no interaction with the incoming waves, permitting these signals to traverse the Frequency Selective Surface (FSS) with negligible attenuation.

The numerical results presented in Fig. 4 delineate the electric field, directivity, and gain for the ON configurations of the MEMS switch.

Noteworthy distortion of the beam is observed in the 20- and 40-degree scans, which can also be attributed to phase errors induced by the combined effects of a large angle of arrival and significant scan angles. The decrease in gain observed during the 20- and 40-degree scans in the azimuth plane is linked to the phenomenon known as angle blindness, a phenomenon also anticipated by simulation models. Cross-polarisation predominantly arises from specular reflections attributed to dipole element mismatches where the MEMS is connected. The role of a 20° scan reflection in the context of a Frequency Selective Surface (FSS) for GNSS L1 and L5 bands is primarily related to beam steering and enhancing coverage, as well as signal suppression for specific directions. The values of gain and electric field are illustrated in each plot, signifying the peak gain, sidelobe level, and cross-polarisation (measured between co-polar and cross-polar peaks), respectively. Theoretical values reveal similar trends in both mechanical deflection and frequency-response measurements, with the level of deflection attained satisfying the requirements for successfully demonstrating the duplexing of a signal and the FSS tuning characteristics initially proposed in this project. Typically, gain deviations of ±3 dB from the design values are anticipated, especially during beam scanning. The design parameters will influence the extent of fluctuation. For example, in gain design, the feed beamwidth, edge taper, and feed distribution efficiency must be considered; increasing the feed beamwidth (or altering the F/D ratio) will lead to a decrease in gain. By tuning or reconfiguring the FSS (using MEMS switches), the reflected beam can be directed at a 20° angle from the normal (broadside). This means that instead of reflecting GNSS signals (at L1: 1.575 GHz and L5: 1.176 GHz) straight back, the FSS can steer the reflected signals to a particular direction, which is useful for improving signal reception in receivers placed at an angle and suppressing multipath interference by redirecting unwanted reflections away from sensitive areas. This is useful for applications such as smart antennas, filtering out non-GNSS signals, and preventing interference.

4 Conclusion

In conclusion, this study presents a significant advancement in the design of Frequency Selective Surfaces (FSS), utilising Micro-Electro-Mechanical Systems (MEMS) switches for enhanced control over dipole elements integrated within the substrate. The development of reconfigurable FSS marks a notable contribution to the field, particularly in improving tuning capabilities for L1 band navigation frequencies. A thorough numerical evaluation of a 9×9 array of frequency-selective surfaces demonstrates the potential for versatile two-dimensional beamforming applications. However, the complexities associated with the design, modelling, and characterisation of reflect arrays must be acknowledged, as they are compounded by the interplay of desired and undesired (specular) reflections on the radiating facet of the array. Preliminary experiments have validated the efficacy of the proposed FSS design, underscoring the advantages afforded by MEMS integration. Furthermore, the capability for multi-frequency operation is crucial in enabling the simultaneous transmission and reception of communication signals. The simulated performance patterns align closely with the empirical results, reinforcing the reliability of the findings and their implications for future applications of Frequency Selective Surfaces across various domains.

Author contributions M.M authored the primary manuscript with oversight from M.D, while I.D.C revised the manuscript and developed the mathematical sections. G.T and J.I designed the essential MEMS switch needed for the antenna and executed the full MEMS design. M.M conducted the simulation design and analysed the numerical outcomes. K.G reviewed the entire manuscript and offered suggestions for enhancement.

Funding Open access funding provided by Università degli Studi di Trento within the CRUI-CARE Agreement.

Data availability No datasets were generated or analysed during the current study.

Declarations

Conflict of interest The authors declare no conflict of interests.

References

Ansari A (2019) 'Single Crystalline Scandium Aluminum Nitride: An Emerging Material for 5G Acoustic Filters', in *2019 IEEE MTT-S International Wireless Symposium (IWS)*, Guangzhou, China: IEEE, May pp. 1–3. https://doi.org/10.1109/IEEE-IWS.2019.8804148

Assylbekova M, Pirro M, Zhao X, Michetti G, Simeoni P, Rinaldi M (2023) 'Study of the Performance Enhancement of Sc-Doped AlN Super High Frequency Cross-Sectional Lamé Mode Resonators.' Micromachines 14(3):515. https://doi.org/10.3390/mi14030515

Barrera O et al (2024) 'Transferred Thin Film Lithium Niobate as Millimeter Wave Acoustic Filter Platforms', in., *IEEE 37th International Conference on Micro Electro Mechanical Systems (MEMS)*, Austin, TX, USA: IEEE, Jan. 2024, pp. 23–26. https://doi.org/10.1109/MEMS58180.2024.10439593

Barlevy AS, Rahmat-Samii Y (1999) Control of resonant bandwidth in frequency-selective surfaces by tilting the periodic elements. Microw Opt Technol Lett 21(2):114–117

Coutts GM, Mansour RR, Chaudhuri SK (2007) A MEMS-Tunable Frequency-Selective Surface Monolithically Integrated on a Flexible Substrate, in 2007 IEEE/MTT-S International Microwave Symposium}, Jun. pp. 497–500

Chen L et al (2023) 'Scandium-Doped Aluminum Nitride for Acoustic Wave Resonators, Filters, and Ferroelectric Memory Applications.' ACS Appl Electron Mater 5(2):612–622. https://doi.org/10.1021/acsaelm.2c01409

Cheng C-C, Abbaspour-Tamijani A (2009) Evaluation of a novel topology for MEMS programmable reflectarray antennas. IEEE Trans Microwave Theory Tech 57(12):3333–3344

Farooq U (2021) C-band and X-band switchable frequency-selective surface. Electronics 10(4):476

Hakim F, Rudawski N, Tharpe T, Tabrizian R (2023) The Ferroelectric-Gate fin microwave acoustic signal processor. Mar 29. https://doi.org/10.21203/rs.3.rs-2544285/v1

Izhar et al 'Periodically poled aluminum scandium nitride bulk acoustic wave resonators and filters for communications in the 6G Era', May 24, 2024, *arXiv*: arxiv:2406.15431. https://doi.org/10.48550/arXiv.2406.15431

Ghosh S, Srivastava KV, Dual-Band A (2020) Tunable Frequency Selective Surface With Independent Wideband Tuning, Antennas and Wireless Propagation Letters, vol. 19, no. 10, pp. 1808–1812, Oct

Kiani GI, Bird TS, Chan KY (2011) MEMS enabled frequency selective surface for 60 GHz applications, in 2011 IEEE International Symposium on Antennas and Propagation (APSURSI)}, Jul. pp. 2268–2269

Kim K, Phon R, Park E, Lim S (2024) '4D-printed intelligent reflecting surface with improved beam resolution via both phase modulation and space modulation.' Microsyst Nanoeng 10(1):1–9

Loebl HP, Metzmacher C, Milsom RF, Lok P, Van Straten F, Tuinhout A (Jan. 2004) RF bulk acoustic wave resonators and filters. J Electroceram 12:1–2. https://doi.org/10.1023/B:JECR.0000034005.21609.91

Mamedes DF, Bornemann J (2021) 'High-Gain Reconfigurable Antenna System Using PIN-Diode-Switched Frequency Selective Surfaces for 3.5 GHz 5G Application', in 2021 SBMO/IEEE MTT-S International Microwave and Optoelectronics Conference (IMOC), Fortaleza, Brazil: IEEE, Oct. pp. 1–3

Mansutti G, Mobashsher AT, Bialkowski K, Mohammed B, Abbosh A (2020) Millimeter-wave substrate integrated waveguide probe for skin cancer detection. IEEE Trans Biomed Eng 67(9):2462–2472

Munk BA (2000) Frequency selective surfaces: theory and design, 1st edn. Wiley

Rana B, Cho S-S, Hong I-P (2023) Review paper on hardware of reconfigurable intelligent surfaces. IEEE Access 11:29614–29634

Safari M, Shafai C, Shafai L (2015) X-band tunable frequency selective surface using MEMS capacitive loads. IEEE Trans Antennas Propag 63(3):1014–1021

Schoenlinner B, Abbaspour-Tamijani A, Kempel LC, Rebeiz GM (2004) Switchable low-loss RF MEMS Ka-band frequency-selective surface. IEEE Trans Microw Theory Tech 52(11):2474–2481

Sharma S, Prajapati PR (2022) Detection of Skin Abnormalities using a Highly Sensitive Planar Microstrip Probe, 2022 IEEE Wireless Antenna and Microwave Symposium (WAMS), pp. 1–5

Stettler S, Villanueva LG (2025) 'Suspended lithium niobate acoustic resonators with Damascene electrodes for radiofrequency filtering.' Microsyst Nanoeng 11(1):131. https://doi.org/10.1038/s41378-025-00980-w

Yang K et al (2024) Nanosheet lithium niobate acoustic resonator for MmWave frequencies. IEEE Electron Device Lett 45(2):272–275. https://doi.org/10.1109/LED.2023.3345345

Zendejas JM, Gianvittorio JP, Rahmat-Samii Y, Judy JW (2006) Magnetic MEMS reconfigurable frequency-selective surfaces. J Microelectromech Syst 15(3):613–623